

See discussions, stats, and author profiles for this publication at: <https://www.researchgate.net/publication/263959052>

Structural Diversity in a Copper(II)/Isophthalato/9-Methyladenine System. From One- to Three-Dimensional Metal-Biomolecule Frameworks

ARTICLE in CRYSTAL GROWTH & DESIGN · JUNE 2013

Impact Factor: 4.89 · DOI: 10.1021/cg400458a

CITATIONS

8

READS

39

6 AUTHORS, INCLUDING:



Garikoitz Beobide

Universidad del País Vasco / Euskal Herriko U...

54 PUBLICATIONS 711 CITATIONS

SEE PROFILE



Oscar Castillo

Universidad del País Vasco / Euskal Herriko U...

131 PUBLICATIONS 1,969 CITATIONS

SEE PROFILE



Javier Cepeda

Universidad del País Vasco / Euskal Herriko U...

33 PUBLICATIONS 280 CITATIONS

SEE PROFILE



Pascual Roman

Universidad del País Vasco / Euskal Herriko U...

192 PUBLICATIONS 3,049 CITATIONS

SEE PROFILE

Structural Diversity in a Copper(II)/Isophthalato/9-Methyladenine System. From One- to Three-Dimensional Metal-Biomolecule Frameworks

Sonia Pérez-Yáñez,* Garikoitz Beobide, Oscar Castillo,* Javier Cepeda, Antonio Luque, and Pascual Román

Departamento de Química Inorgánica, Facultad de Ciencia y Tecnología, Universidad del País Vasco, UPV/EHU, Apartado 644, E-48080 Bilbao, Spain

S Supporting Information

ABSTRACT: The synthesis, X-ray single crystal structure analyses, and physicochemical characterization of copper(II)-isophthalato coordination polymers containing the 9-methyladenine nucleobase $\{[\text{Cu}(\mu\text{-iso})(9\text{Meade})(\text{H}_2\text{O})_2]\}_n$ (**1**), $\{[\text{Cu}(\mu\text{-iso})(\mu\text{-}9\text{Meade})]\}_n$ (**2**), $\{[\text{Cu}_2(\mu_4\text{-iso})_2(9\text{Meade})_2]\cdot 2\text{H}_2\text{iso}\}_n$ (**3**), $\{[\text{Cu}_2(\mu_3\text{-iso})_2(\mu\text{-}9\text{Meade})(\text{H}_2\text{O})]\cdot \text{H}_2\text{O}\}_n$ (**4**), and $\{[\text{Cu}_2(\mu_3\text{-iso})_2(\mu\text{-}9\text{Meade})(\text{H}_2\text{O})_2]\cdot 1.5\text{H}_2\text{O}\}_n$ (**5**) (where iso = isophthalato and 9Meade = 9-methyladenine) are reported. Compound **1** contains neutral chains in which the isophthalato dianion acts as a bridging ligand, while the methylated nucleobase behaves as N7-coordinated terminal ligand. Compound **2** exhibits a two-dimensional network in which the aromatic dicarboxylate ligand and the nucleobase act as bidentate bridging ligands. Compound **3** is based on dimeric paddle-wheel shaped entities in which the copper(II) atoms are bridged by means of four isophthalato ligands to give a NO_4 chromophore with the N7 nitrogen atom of the 9-methyladenine filling the axial position. The linkage of the dimeric entities through the second carboxylate group of the dianions leads to covalent layers that are further connected to give a supramolecular three-dimensional pillared structure by means of hydrogen bonding and $\pi\text{-}\pi$ interactions involving noncoordinated isophthalic acid molecules. Compounds **4** and **5** contain paddle-wheel $[\text{Cu}_2(\mu\text{-iso})_4(9\text{Meade})_2]$ entities and $[\text{Cu}(\text{H}_2\text{O})]$ or $[\text{Cu}(\text{H}_2\text{O})_2]$ units connected by means of the isophthalate and 9-methyladenine bidentate bridging ligands.

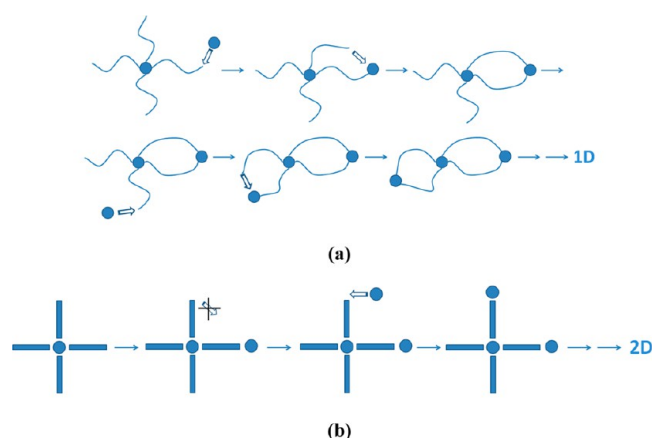
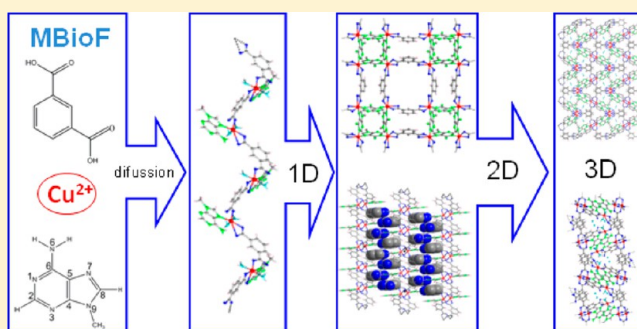


Figure 1. Schematic representation showing the assembly process of paddle-wheel dimeric entities (circles) with (a) flexible dicarboxylate (bent lines) and (b) rigid linear ligands (sticks).

INTRODUCTION

Design of coordination frameworks via deliberate selection of metals and multifunctional ligands, including biological relevant molecules such as nucleobases,¹ is one of the most attractive topical areas of chemistry due to their fascinating structural diversity and their development as new materials with tunable properties.² An essential part of coordination polymer design, and the wider field of crystal engineering, is the use of building blocks that combine the flexibility and necessary interconnection capability to achieve the desired dimensionality, but also the sufficient strength to permit a predictable core which maintains their structural integrity throughout the construction of the solid. In this sense, $[\text{M}_2(\mu\text{-L})_4\text{X}_2]$ entities have been known for a long time since the crystal structure of the $[\text{Cu}_2(\mu\text{-acetato})_4(\text{H}_2\text{O})_2]$ compound was reported.³ The attractiveness of the paddle-wheel (PW) motif is that structural and functional changes can be achieved almost at will by simply varying the metal cores, the bridging moieties, or the X-

Received: March 27, 2013

Revised: May 27, 2013

Published: May 27, 2013

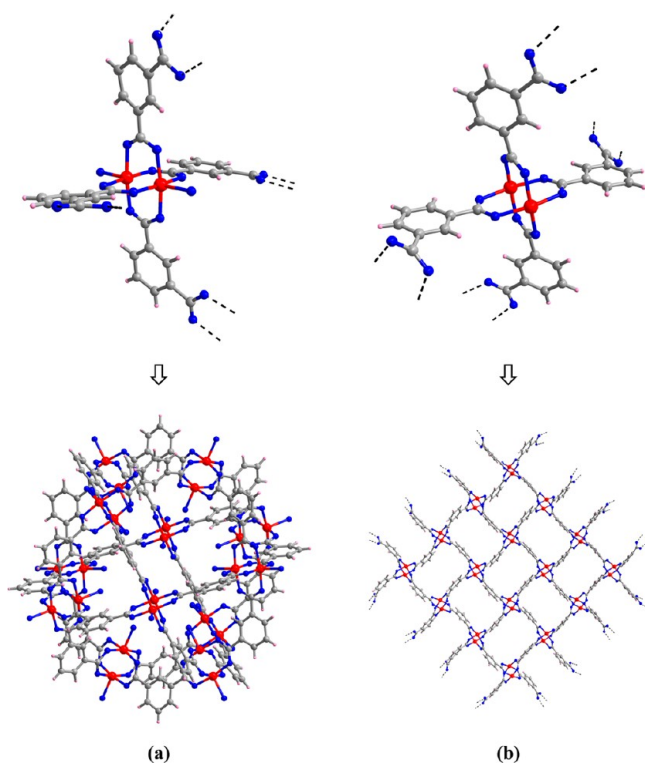


Figure 2. Structures based on $[\text{Cu}_2(\mu\text{-isophthalato})_4]$ dimeric entities: (a) non-centrosymmetric dimer giving rise to clusters and (b) centrosymmetric dimer rendering layers.

ligands.⁴ These axial positions, usually occupied by solvent molecules, can be replaced by nucleobase ligands, thus increasing the ability of the systems to be involved in molecular

recognition processes. The functional versatility of the dinuclear PW motifs makes them particularly suitable as secondary building units (SBUs) for the design and synthesis of numerous crystalline materials ranging from zero-dimensional (0D) species to three-dimensional (3D) coordination polymers with interesting properties in areas such as magnetism, medicine, catalysis, and gas storage.^{2,5,6}

Continuing our previous work based on the use of dicopper PW entities built up from adenine nucleobase and carboxylato ligands, we have designed and synthesized five new compounds employing 9-methyladenine as the nucleobase and benzene-1,3-dicarboxylic acid (isophthalic acid) as the carboxylato ligand precursor.

Aromatic spacers provide greater rigidity because their geometric characteristics are limited, allowing restriction of the structural variability. Furthermore, these ligands provide the system the ability to modify or functionalize the channels without altering the 3D framework. An example of this strategy is the isorecticular diversity of the family of compounds derived from the MOF-5, $[\text{Zn}_4\text{O}(\text{benzene-1,4-dicarboxylate})_3]$, wherein the replacement of the dicarboxylic acid ligand by longer spacers or the modification with different functional groups, without modifying the disposition of the carboxylate groups, allows an increase of the pore size and/or functionalization of the walls thereof.⁷ Furthermore, the use of rigid aromatic dicarboxylates in conjunction with adenine and different metals, such as zinc or nickel, has demonstrated the suitability for obtaining permanent porous structures.⁸ In the particular case of PW shaped dimeric units, the use of aromatic dicarboxylic ligands allows structures to be obtained ranging from isolated clusters to porous 3D systems, as well as mono- and two-dimensional (2D) systems.⁹

Taking advantage of the specific $[\text{Cu}_2(\mu\text{-dicarboxylato})_4(\text{X})_2]$ dimeric entity, it bears mentioning that when using

Table 1. Crystallographic Data and Structure Refinement Details of Compounds 1–5

	1	2 ^a	3	4	5 ^b
empirical formula	$\text{C}_{14}\text{H}_{15}\text{CuN}_5\text{O}_6$	$\text{C}_{14}\text{H}_{11}\text{CuN}_5\text{O}_4$	$\text{C}_{44}\text{H}_{34}\text{Cu}_2\text{N}_{10}\text{O}_{16}$	$\text{C}_{22}\text{H}_{19}\text{Cu}_2\text{N}_5\text{O}_{10}$	$\text{C}_{22}\text{H}_{19}\text{Cu}_2\text{N}_5\text{O}_{11.5}$
formula weight	412.85	376.82	1085.90	640.51	667.53
crystal system	monoclinic	tetragonal	monoclinic	monoclinic	triclinic
space group	$P2_1/c$	$P4_2/c$	$P2_1/a$	$P2_1/a$	$P\bar{1}$
<i>a</i> (Å)	9.289(4)	16.6280(4)	13.458(2)	9.628(1)	9.2360(4)
<i>b</i> (Å)	10.210(5)	16.6280(4)	13.046(1)	19.315(1)	12.4650(7)
<i>c</i> (Å)	17.241(7)	11.0490(5)	13.826(2)	14.872(1)	23.2130(9)
α (°)	90	90	90	90	90.297(4)
β (°)	99.938(3)	90	96.922(12)	108.705(3)	96.642(4)
γ (°)	90	90	90	90	104.656(4)
<i>V</i> (Å ³)	1611(1)	3054.9(2)	2409.9(6)	2619.6(2)	2566.5(2)
<i>Z</i>	4	8	2	4	4
ρ_{calcd} (g cm ^{−3})	1.703	1.639	1.496	1.624	1.727
μ (mm ^{−1})	1.402	1.460	0.963	1.687	2.695
reflections collected	12192	10369	13662	40063	19325
unique data/parameters	3408/236	3301/120	4240/321	7084/339	9044/715
<i>R</i> _{int}	0.0471	0.0404	0.1358	0.0343	0.0828
goodness of fit (<i>S</i>) ^c	0.929	1.071	0.894	1.041	0.951
<i>R</i> ₁ ^d / <i>wR</i> ₂ ^e [<i>I</i> > 2σ(<i>I</i>)]	0.0395/0.0932	0.1286/0.2582	0.1050/0.2571	0.0628/0.1621	0.0614/0.1566
<i>R</i> ₁ ^d / <i>wR</i> ₂ ^e [all data]	0.0559/0.0979	0.1420/0.2662	0.2040/0.3001	0.0748/0.1688	0.0939/0.1736

^a9-Methyladenine bridging ligand is disordered into two coplanar arrangements with inverted orientation regarding the coordination mode ($\mu\text{-}1\kappa\text{N}1:2\kappa\text{N}7/\mu\text{-}1\kappa\text{N}7:2\kappa\text{N}1$). ^bNonmerohedral twin with a twin law of (1.0035 0.0019 0.0162/−0.0005 0.9996 0.0001/−0.1129 −0.0205 0.9941) and a percentage of the minor domain of 29%. ^c $S = [\sum w(F_o^2 - F_c^2)^2 / (N_{\text{obs}} - N_{\text{param}})]^{1/2}$. ^d $R_1 = \sum ||F_o| - |F_c|| / \sum |F_o|$. ^e $wR_2 = [\sum w(F_o^2 - F_c^2)^2 / \sum wF_o^2]^{1/2}$; $w = 1/[\sigma^2(F_o^2) + (aP)^2 + bP]$ where $P = (\max(F_o^2, 0) + 2F_c^2)/3$ with $a = 0.0637$ (1), 0.0001 (2), 0.1589 (3), 0.0809 (4), 0.1066 (5), and $b = 11.3145$ (2).

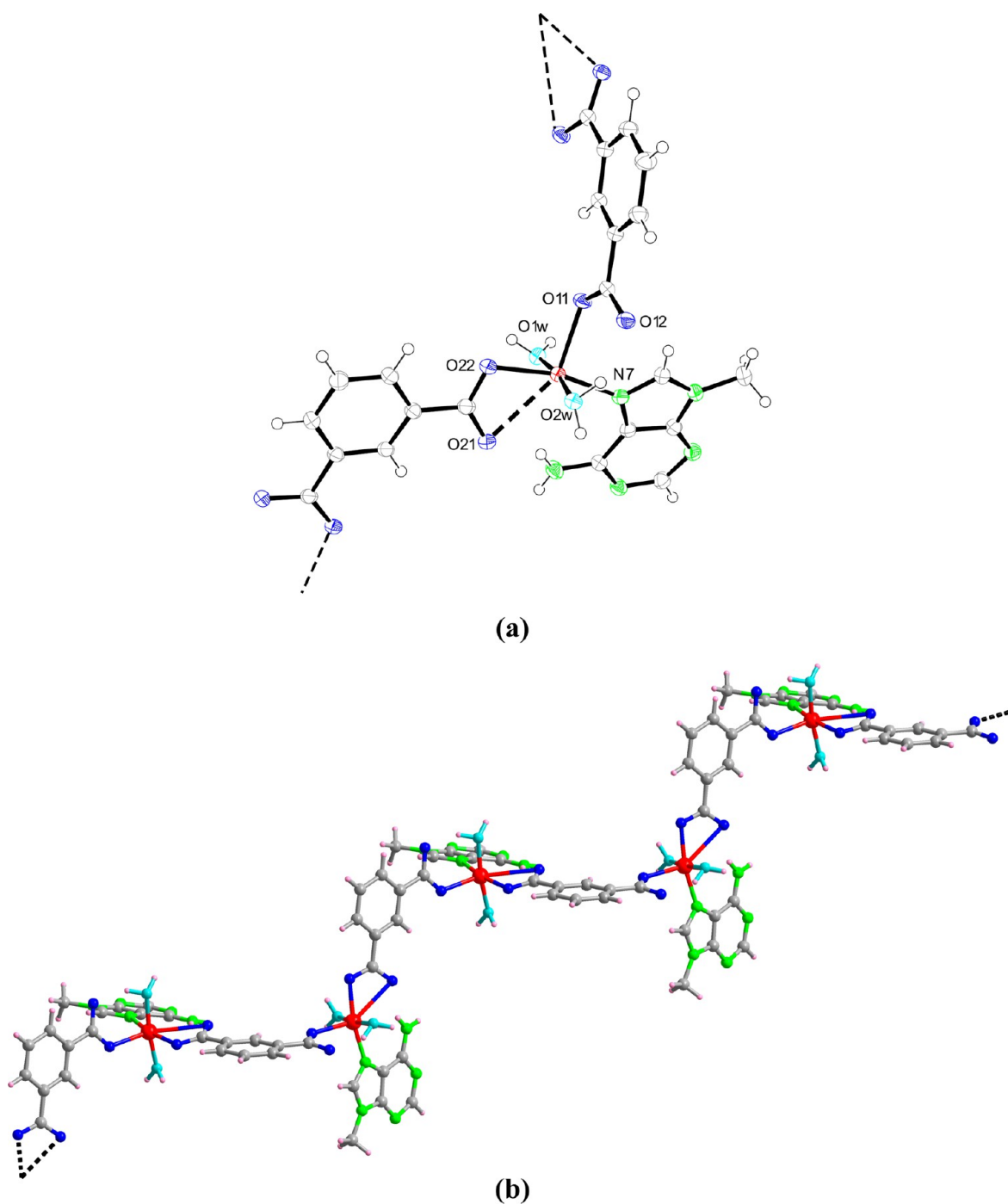


Figure 3. (a) Coordination environment and (b) polymeric chain in compound **1**.

aliphatic dicarboxylic acids, the kinetics of the reaction makes the system to evolve toward one-dimensional (1D) structures.¹⁰ To visualize this effect, we can just imagine two dimeric entities linked by a unique bridging dicarboxylic ligand and think about the behavior of a second dicarboxylic ligand: (i) it can wait until getting close to a third dimeric unit and join it to generate extended 2D or 3D structures, or (ii) it can connect to the already linked second dimeric unit, as it happens in the $\{[\text{Cu}_2(\mu_4\text{-glutarato/pimelato})_2(\text{methyladenine})_2]\}_n$ compounds previously reported by our group.¹⁰ The remaining ligands are opposite oriented to the first and second ones, and, therefore, they have no access to the second dimeric entity, so they must wait until a third unit approximates, and once a dicarboxylato

ligand is bound, the next one will follow it. The repetition of this process generates chains of dimeric units doubly bridged by the dicarboxylic ligands, as it is schematized in Figure 1a.

When rigid aromatic ligands are used, they cannot twist enough to establish a double bridge between the metal centers and the structure evolves toward more complex architectures. In particular for terephthalic acid, a typical example of a bridging ligand in crystal engineering, the coplanar disposition of the carboxylato groups at 180° generates a 2D structure (Figure 1b). However, when this anion is functionalized in the *ortho* position, for instance, the 2-chloroterephthalic ligand, the steric hindrance of the substituents forces the carboxylato groups to be arranged perpendicular, so the metal–organic

polymer grows along the three dimensions leading to a porous framework.¹¹

With regard to the isophthalic acid, two dimeric entities with different relative orientation of the ligands may coexist in solution leading to (a) discrete clusters when the dimer is non-centrosymmetric, with all uncoordinated carboxylate groups pointing toward the same end of the dimer,¹² or (b) infinite layers when the dimeric entity is centrosymmetric, with free carboxylate groups pointing toward both ends (Figure 2).¹³ Usually, discrete entities or crystal structures of lower dimensionality are the kinetically favored product as they are formed by the combination of a smaller number of constituents. However, in order to isolate these kinetically favored structures, they must be insoluble enough to precipitate, preventing the system to evolve toward more extended structures that are thermodynamically more stable.

In all these systems, if the apical position of the dimeric entities is filled by a bridging ligand, the resulting structure increases its connectivity achieving even a 3D coordination network.¹⁴ In any case, it is well recognized that the crystal engineering of coordination polymers with desired structures and specific properties still remains a difficult challenge, since there is a variety of factors influencing the self-assembly process, such as the coordination geometry and the oxidation state of the metal ions, metal-to-ligand ratio, solvents, temperature, and/or counterions.

EXPERIMENTAL SECTION

Synthesis. A mixture of single crystals of compounds 1–5 was obtained by slow diffusion of a methanolic solution (5 mL) of $\text{Cu}(\text{NO}_3)_2 \cdot 3\text{H}_2\text{O}$ (0.2 mmol, 0.0483 g) into an aqueous-methanolic solution (1:1, 10 mL) of 9-methyladenine (0.2 mmol, 0.0307 g) and isophthalic acid (0.2 mmol, 0.0336 g). The diffusion of the reactants generates different concentrations and stoichiometric conditions, which gives rise to a mixture of crystals stratified along the diffusion tube after several weeks. The similar morphology and color of the crystals of compounds 1–5 have prevented their manual separation. All attempts to achieve pure samples of each compound have been unsuccessful except for compound 1 which has been obtained by direct mixture of reactants in aqueous-methanolic solution. Yield: 80–90%. Anal. Calcd for $\{[\text{Cu}(\mu\text{-iso})(9\text{Meade})(\text{H}_2\text{O})_2]\}_n$ (1), $\text{C}_{14}\text{H}_{15}\text{CuN}_5\text{O}_6$ (412.85 g/mol): C, 40.73; H, 3.66; N, 16.96; Cu, 15.39%. Found: C, 40.99; H, 3.41; N, 17.12; Cu, 15.11%. IR (cm^{-1} , KBr pellet): 3380m for $\nu(\text{O-H})$; 3320m for $(\nu(\text{NH}_2) + 2\delta(\text{NH}_2))$; 3120m for $\nu(\text{C}_8\text{-H} + \text{C}_2\text{-H} + \text{NH}_2) + \nu(\text{C-H})_{\text{iso}}$; 2920m for $\nu(\text{CH}_3)$; 1688s for $\nu_{\text{as}}(\text{O-C-O})$; 1602s for $(\nu(\text{C}=\text{C}) + \delta(\text{NH}_2))$; 1583m for $\nu(\text{C}_4\text{-C}_5)$; 1550s for $\nu(\text{N}_3\text{-C}_4\text{-C}_5)$; 1492w, 1475w, 1443w, 1431w for $(\delta(\text{C}_2\text{-H} + \text{C}_8\text{-N}_9) + \nu(\text{C}_8\text{-H}))$; 1415w for $\delta(\text{N}_1\text{-C}_6\text{-H}_6)$; 1387w, 1374m, 1338w for $\nu(\text{C}_5\text{-N}_7\text{-C}_8)$; 1302w, 1272w, 1249w, 1238w for $(\nu(\text{N}_9\text{-C}_8 + \text{N}_3\text{-C}_2) + \delta(\text{C-H}) + \nu_s(\text{O-C-O}))$; 1188w, 1161w for $(\delta(\text{C}_8\text{-H}) + \nu(\text{N}_7\text{-C}_8))$; 1068m, 1004w, 961w for $\tau(\text{NH}_2)$; 931w, 908w, 897w for $(\nu(\text{N}_1\text{-C}_6) + \tau(\text{NH}_2))$; 836w, 794w, 762w, 737m, 727m, 721m for $\delta(\text{O-C-O})$; 653w, 591m for ring deformation; 572w, 539w, 519w, 467w, 440w, 416w for $\nu(\text{M-O} + \text{M-N})$.

X-ray Diffraction Data Collection and Structure Determination. Diffraction data of single crystals were collected at 100(2) K on a STOE IPDS (1, 3, 4) and on an Oxford Diffraction Xcalibur (2) diffractometer with graphite-monochromated Mo $K\alpha$ radiation ($\lambda = 0.71073$ Å), and on a Supernova (5) diffractometer Cu $K\alpha$ radiation ($\lambda = 1.5418$ Å). The data reduction was done with the X-RED¹⁵ and CrysAlis RED¹⁶ programs, respectively. Structures were solved by direct methods using the SIR92 program¹⁷ and refined by full-matrix least-squares on F^2 including all reflections (SHELXL97).¹⁸ All calculations were performed using the WINGX crystallographic software package.¹⁹ Crystal data and details of the refinement parameters of the compounds are given in Table 1.

RESULTS AND DISCUSSION

Crystal Structure of $\{[\text{Cu}(\mu\text{-iso})(9\text{Meade})(\text{H}_2\text{O})_2]\}_n$ (1). Compound 1 contains neutral chains in which the isophthalic

Table 2. Selected Bond Lengths (Å) of Compound 1

Cu1–N7	2.030(3)	Cu1–O22	2.000(2)
Cu1–O11	2.189(2)	Cu1–O1w	1.963(2)
Cu1–O21	2.724(2)	Cu1–O2w	1.976(2)

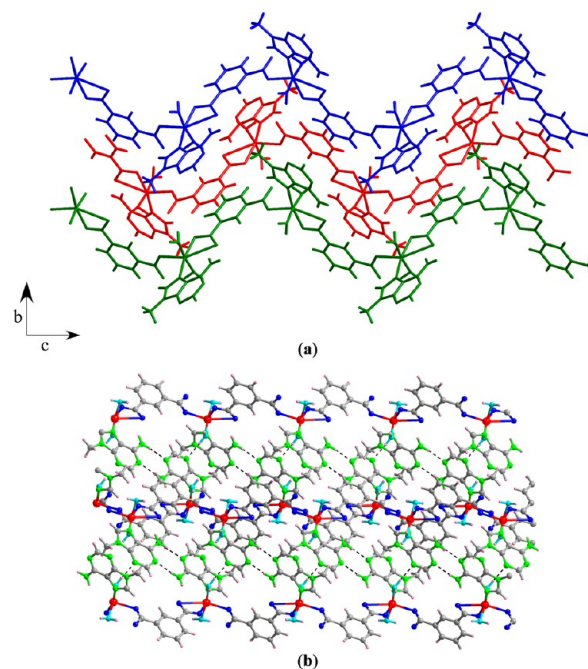


Figure 4. (a) Layer of chains and (b) hydrogen bonding interactions between Watson–Crick faces in compound 1.

Table 3. Selected Bond Lengths (Å) of Compound 2^a

Cu1–N1	2.140(11)	Cu1–O12a	1.784(12)
Cu1–N7b	2.056(12)	Cu1–O21	2.140(10)
Cu1–O11a	2.660(9)	Cu1–O22	2.119(11)

^aSymmetry codes: (a) $y, -x + 2, -z$; (b) $y, -x + 1, -z$.

ligand bridges two metal centers with a $\kappa^2\text{O}, \text{O}'\text{:}\kappa\text{O}''$ coordination mode, while 9-methyladenine acts as terminal ligand (Figure 3). The copper(II) atom shows a distorted 4 + 1 coordination environment in which the basal plane consists of the O22 oxygen atom of the isophthalic ligand, the imidazolic N7 atom of the 9-methyladenine, and two water molecules in trans arrangement. The metal coordination sphere is filled by one of the oxygen atoms of each carboxylate group of the isophthalic ligand (O11 and O21) through the axial positions with Cu–O bond distances substantially longer than the equatorial ones due to the Jahn–Teller distortion (Table 2). In fact, the coordination bond distance involving O21 oxygen atom is so long (2.724 Å) that the continuous shape measurements²⁰ result in a coordination geometry closer to a square pyramid ($S_{\text{SPY}} = 0.58$) than to an octahedron ($S_{\text{Oh}} = 4.55$).

The asymmetric coordination of the two carboxylate groups of the isophthalic ligand generates zigzag chains spreading along the c axis, where the equatorial planes of two consecutive chromophores are rotated 90°. The exocyclic amino group of

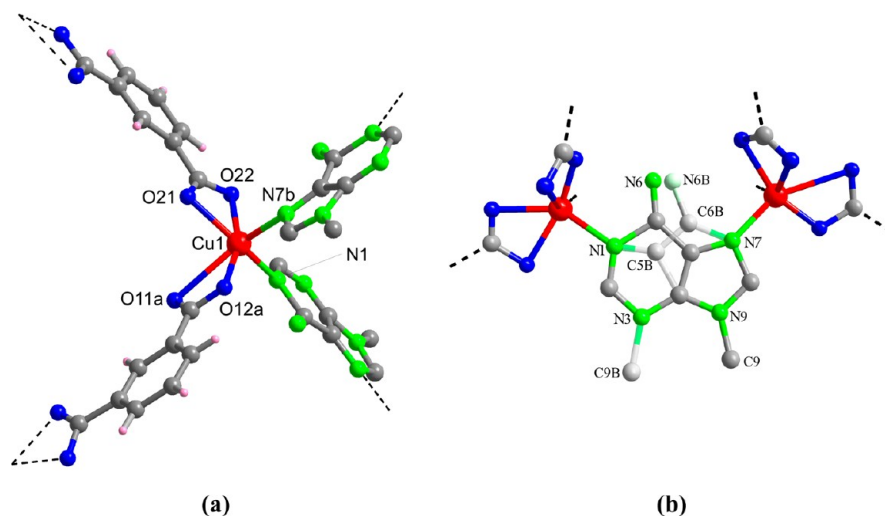


Figure 5. (a) Cu(II) coordination environment and (b) coplanar disorder of the 9-methyladenine in compound 2.

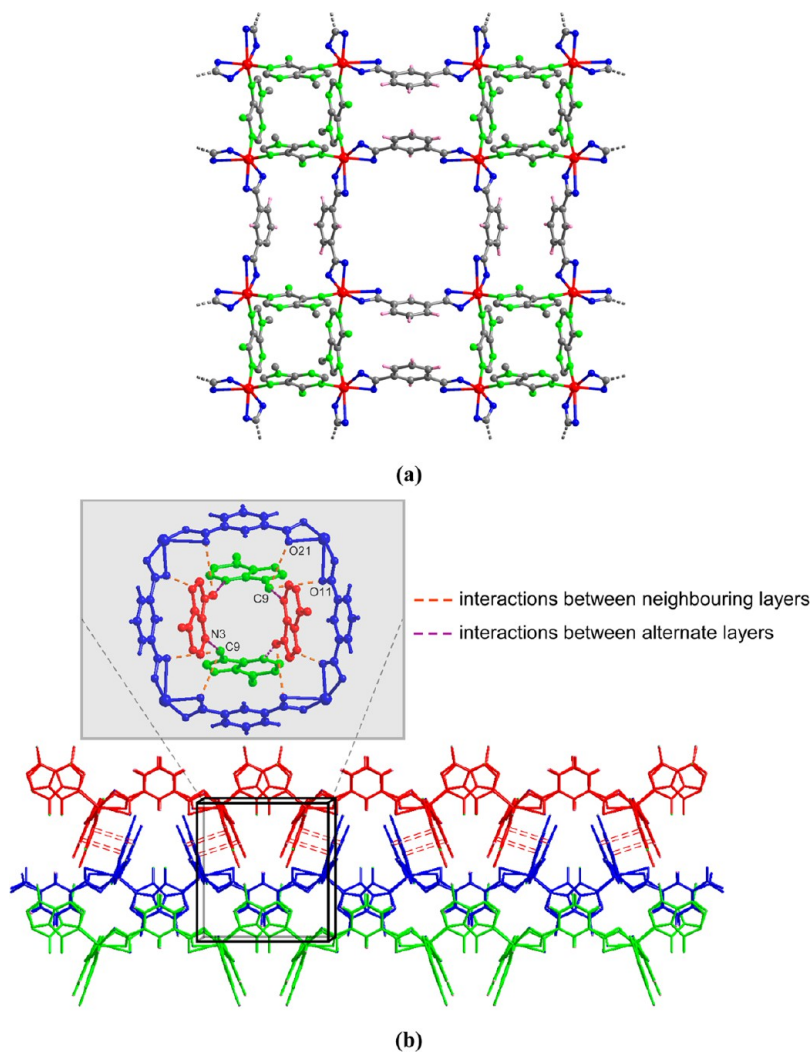


Figure 6. (a) View of the rectangular layer throughout the crystallographic [001] direction and (b) stacking along the *a* axis showing the interactions between the layers in compound 2.

the 9-methyladenine molecule forms an intramolecular hydrogen bonding interaction with the O21 oxygen atom of the isophthalic ligand. Moreover, the O2w crystallization water molecule also establishes an intramolecular hydrogen bond with

the noncoordinated O12 oxygen atom. The chains are linked through hydrogen bonding interactions between the coordination water molecules and the O12 and O21 oxygen atoms of the dicarboxylate, giving rise to layers that are spreading along

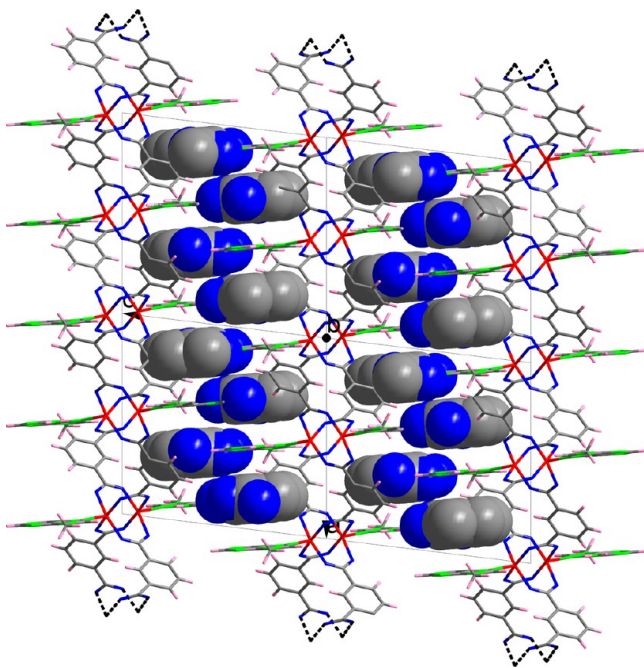


Figure 7. Layers of compound 3 showing the isophthalic acid molecules inserted among them.

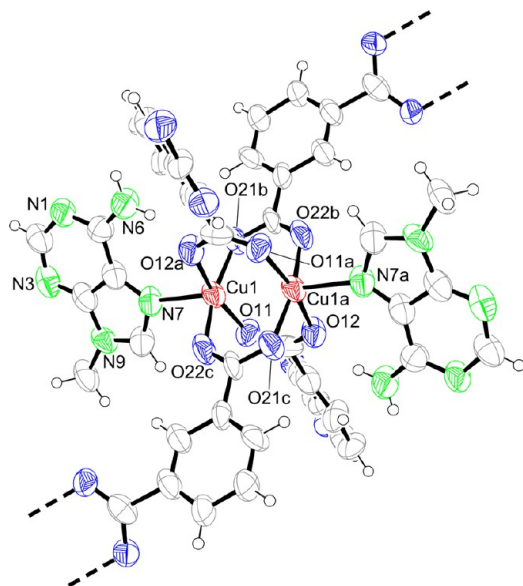


Figure 8. Dimeric entity of compound 3.

Table 4. Selected Bond Lengths (Å) of Compound 3^a

Cu1–N7	2.161(10)	Cu1–O21b	1.948(8)
Cu1–O11	1.952(8)	Cu1–O22c	1.968(9)
Cu1–O12a	1.975(8)	Cu1...Cu1a	2.682(3)

^aSymmetry codes: (a) $-x, -y + 1, -z$; (b) $-x + 1/2, y + 1/2, -z$; (c) $x - 1/2, -y + 1/2, z$.

the *bc* plane, as it is shown in Figure 4. These layers are held together by means of a double N6–H...N1 hydrogen bonding interaction between the Watson–Crick faces of the terminal nucleobases and a hydrogen bonding interaction between the N3 atom of the 9-methyladenine and the O1w water molecule. The crystal cohesiveness is reinforced by π – π interactions

between the aromatic rings of the 9-methyladenine and isophthalato ligand (see Supporting Information).

Crystal Structure of $\{[\text{Cu}(\mu\text{-iso})(\mu\text{-9Meade})]\}_n$ (2).

Compound 2 is built up from the stacking of metal–organic layers in which the copper atoms are bridged by bisbidentate isophthalato dianions and bidentate 9-methyladenine ligands. The copper(II) atom is hexacoordinated to four oxygen atoms belonging to two carboxylato groups and two nitrogen atoms of two 9-methyladenine molecules (Table 3) to give a *cis*-CuO₄N₂ donor set with a distorted octahedral geometry ($S_{\text{Oh}} = 7.57$) due to the acute bite angle of the two chelating rings (ca. 55°). As it is shown in Figure 5, the bridging 9-methyladenine ligand is disordered into two coplanar positions showing the most usual bidentate mode for this nucleobase, $\mu\text{-}\kappa\text{N1}:\kappa\text{N7}$,²¹ but with a reverse orientation, $\mu\text{-}\kappa\text{N1}:\kappa\text{N7}$ and $\mu\text{-}\kappa\text{N7}:\kappa\text{N1}$.

The coexistence of two bridging ligands results in a 2D network with three metal–organic rings: (i) 10 Å × 10 Å squares formed by four isophthalato ligands, (ii) 10 Å × 7 Å rectangles built by two isophthalato ligands and two 9-methyladenine molecules, and (iii) 7 Å × 7 Å squares with four 9-methyladenine molecules (Figure 6a). This 2D arrangement corresponds to the Shubnikov tetragonal *sql* topology, the point symbol being (4⁴.6²).²² The offset stacking of these layers along the [001] crystallographic direction is sustained by means of π – π interactions involving the isophthalato and the 9-methyladenine ligands with ...ABAB... packing sequence (Figure 6b).

Crystal Structure of $\{[\text{Cu}_2(\mu_4\text{-iso})_2(9\text{Meade})_2]\cdot 2\text{H}_2\text{O}\}_n$ (3).

Compound 3, unlike compounds 1 and 2, is built from the linkage of dimeric PW shaped entities. As described in Figure 2, there are two types of possible structures with isophthalato containing PW units: isolated octahedral clusters and infinite 2D systems. The coordination of the 9-methyladenine to the apical position in the dimeric unit of compound 3 precludes the formation of the octahedral cluster since it would imply the presence of six of these nucleobases in the central cavity of the hexamer with a diameter of ca. 10 Å, for which there is not enough void. Therefore, the generated structure comprises infinite layers among which noncoordinated isophthalic acid molecules are inserted (Figure 7). Each dimeric entity, sited in an inversion center, consists of four isophthalato ligands that bridge the copper(II) atoms and two 9-methyladenine molecules coordinated in the axial positions through the N7 nitrogen atom (Figure 8). The pentacoordinated copper(II) atom shows a square pyramidal environment ($S_{\text{SPY}} = 0.39$) with equatorial distances of ca. 1.96 Å and a slightly greater axial distance of 2.16 Å (Table 4).

The second carboxylato group of the isophthalato ligand connects two adjacent dimeric entities to lead to a 2D network of square rings, with a Shubnikov tetragonal *sql* topology and a (4⁴.6²) point symbol, as it is shown in Figure 9a. For the construction of this network, one of the carboxylato groups is rotated ca. 40° with respect to the mean plane of the ring. This rotation is transferred to the relative orientation between adjacent dimeric entities so that the rings of the layer are not planar but they acquire certain corrugation (Figure 9b).

The 9-methyladenine ligand forms an intramolecular N6–H...O12 hydrogen bonding interaction, and it is disposed outward the layer to interact with the solvate isophthalic acid molecules which act as supramolecular linkers between the layers. These inclusion molecules use one of the carboxylic groups to establish a R₂²(8) hydrogen bonding ring with the Watson–Crick face of a nucleobase, whereas the other one

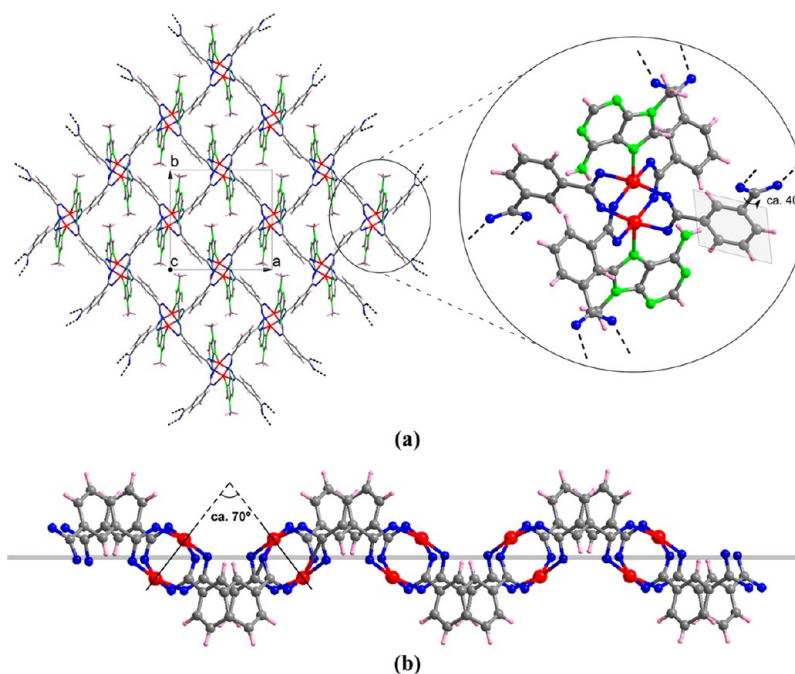


Figure 9. (a) 2D network showing the rotation of the carboxylato group and (b) relative disposition between the SBUs induced by the corrugation of the isophthalato ligand in compound 3.

Table 5. Selected Bond Lengths (Å) of Compound 4^a

dimeric entity		monomeric entity	
Cu1–N1	2.191(4)	Cu2–N7	2.032(4)
Cu1–O11	1.959(3)	Cu2–O21d	2.116(3)
Cu1–O12a	1.958(3)	Cu2–O22d	1.970(3)
Cu1–O41b	1.983(3)	Cu2–O31	1.940(3)
Cu1–O42c	1.994(3)	Cu2–O1w	2.167(4)
Cu1...Cu1a	2.671(1)		

^aSymmetry codes: (a) $-x + 3, -y + 1, -z + 2$; (b) $x + 1/2, -y + 1/2, z$; (c) $-x + 5/2, y + 1/2, -z + 2$; (d) $x - 1/2, -y + 1/2, z - 1$.

interacts with the N3 nitrogen atom of the 9-methyladenine ligand that is anchored to the dimeric entity on the opposite vertex of the square cavity. The supramolecular architecture is reinforced by π – π interactions between the isophthalic acid molecules and the nucleobases.

Crystal Structure of $\{[\text{Cu}_2(\mu_3\text{-iso})_2(\mu\text{-9Meade})(\text{H}_2\text{O})] \cdot \text{H}_2\text{O}\}_n$ (4). The 3D network of 4 is formed by PW shaped $[\text{Cu}_2(\mu\text{-iso})_4(9\text{Meade})_2]$ dimeric entities and $[\text{Cu}(\text{H}_2\text{O})]$ units connected by means of the isophthalate anion and 9-methyladenine. Table 5 gathers coordination distances of the metal centers of both entities.

The copper atom of the dimeric entity exhibits a square pyramidal coordination environment ($S_{\text{SPY}} = 0.36$) in which the

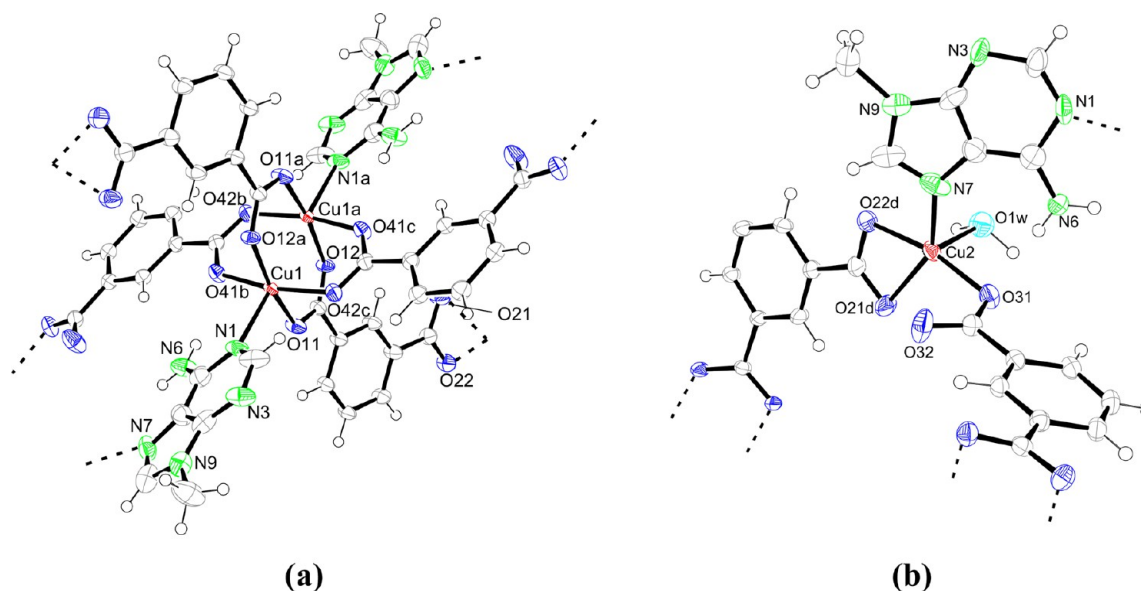


Figure 10. (a, b) Structural entities in compound 4.

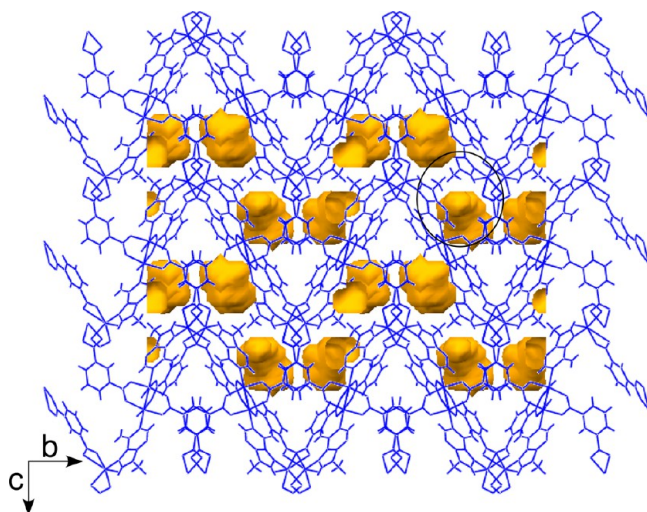


Figure 11. Crystal packing of compound 4 showing the voids filled by crystallization water molecules.

basal plane is occupied by oxygen atoms of four isophthalato ligands. The apical position is filled by the N1 pyrimidinic atom of a 9-methyladenine molecule. The PW entities are connected to the monomeric units by the second carboxylic group of the isophthalato and the imidazolic N7 atom of the nucleobase which acts as bidentate bridging ligand. Two of the isophthalato bridges present a $\mu_3\text{-}\kappa\text{O}:\kappa\text{O}':\kappa^2\text{O}'',\text{O}'''$ coordination mode (where the second carboxylato group chelates the monomeric copper(II) atom), and the two other ones show a $\mu_3\text{-}\kappa\text{O}:\kappa\text{O}':\kappa\text{O}''$ coordination mode with a free oxygen atom. The different coordination modes are reflected in the C–O bond distances which are equivalent for the chelating carboxylato group (1.261, 1.267 Å) and different (1.284, 1.225 Å) for the monodentate carboxylate group. The NO_3Ow donor set in the monomeric entity (Figure 10) is completed with a water molecule to give a distorted square pyramidal geometry ($S_{\text{SPY}} = 2.34$) due to the proximity of the two basal oxygen atoms that form the chelating ring. The 3D binodal network formed by the covalent interactions can be described as a rutile type structure with $(4.6^2)_2(4^2.6^{10}.8^3)$ point symbol.

The 3D architecture is also reinforced by an extensive hydrogen bonding network. The bidentate arrangement of the nucleobase allows the formation of hydrogen bonding rings between the exocyclic amino group and the oxygen atoms of both complex entities. The coordination water molecule of the monomeric entity establishes an $\text{O1w}\cdots\text{H12w}\cdots\text{O32a}$ hydrogen bond with the noncoordinated oxygen atom of the isophthalato ligand and completes its hydrogen bonding scheme with the crystallization water molecule ($\text{O1w}\cdots\text{H11w}\cdots\text{O2w}$). The crystallization molecules occupy discrete voids within the crystal structure that represents 14.8% of the unit cell volume (Figure 11).

Crystal Structure of $\{[\text{Cu}_2(\mu_3\text{-iso})_2(\mu\text{-9Meade})(\text{H}_2\text{O})_2]\cdot 1.5\text{H}_2\text{O}\}_n$ (5). The 3D structure of compound 5 also presents PW shaped $[\text{Cu}_2(\mu\text{-iso})_4(\mu\text{-9Meade})_2]$ dimeric entities linked to $[\text{Cu}(\text{H}_2\text{O})_2]$ units, but it contains two crystallographically independent dimeric entities and two monomeric ones. Besides, the compound presents a higher hydration degree. Figure 12 shows the ORTEP diagrams of the structural units, and Table 6 gathers the bond distances of their coordination environments.

The copper(II) atoms of both dimeric entities (A and B) present a square pyramidal environment ($S_{\text{SPY}} = 0.42$ and 0.52 , respectively), and they are bridged by isophthalato ligands that are asymmetrically coordinated to the monomeric entity: $\mu_3\text{-}\kappa\text{O}:\kappa\text{O}':\kappa^2\text{O}'',\text{O}'''$ (bidentate-chelate) and $\mu_3\text{-}\kappa\text{O}:\kappa\text{O}':\kappa\text{O}''$ (bidentate-monodentate). Both coordination modes coexist in unit A, whereas in unit B the four ligands are bidentate-monodentate ones. The monomeric C entity exhibits a CuNO_3Ow_2 chromophore, ($S_{\text{Oh}} = 5.66$), while the D monomer presents a square pyramidal CuNO_2Ow_2 chromophore ($S_{\text{SPY}} = 0.93$).

The bidentate 9-methyladenine bridging ligand inverts its coordination mode with respect to compound 4, and the nitrogen N7 atom occupies the axial position of the dimeric entities, while the N1 atom completes the coordination sphere of the monomeric centers. The Jahn–Teller effect is enhanced in the monomer with square pyramidal geometry with a longer axial Cu–N distance than in the dimeric entity (2.498 vs 2.205 Å). The 9-methyladenine coordination mode also allows the establishment of a hydrogen bonding interaction between its exocyclic amino group with the dimeric and monomeric entities. The pyrimidinic N3 donor atom of the nucleobase is hydrogen bonded to the coordination water molecules of the $[\text{Cu}(\text{H}_2\text{O})_2]$ entities. $\pi\text{--}\pi$ interactions between the aromatic rings of the nucleobases complete the noncovalent interactions of the crystal building (see Supporting Information).

The overall covalent network also possesses a rutile topology, although the discrete voids occupied by the crystallization water molecules (Figure 13) represent a lower percentage of the total volume than in compound 4 (6.6% vs 14.8%).

Comments on the Cu^{II} /Isophthalato/9-Methyladenine System Diversity. The great structural diversity of this system can be rationalized on the basis of two major factors: (a) the versatility of coordination modes of isophthalato ligand when coordinated to copper(II) metal centers (Figure 14) and (b) the flexible coordination environment of copper(II) atom, probably because of the Jahn–Teller effect, does not impose a unique coordination geometry, and indeed, it can be easily reorganized by slight displacements of the ligands. Moreover, a perusal of the copper(II) containing coordination compounds registered in the CSD shows a similar tendency toward coordination numbers six, five, and four (43, 30, and 27%, respectively).²³ In the present case, both facts imply the coexistence of a handful of coordination moieties in the reaction media which can yield a variety of crystal structures hindering the predictability.

The combination of these factors is evidenced along the herein presented compounds, which is further transferred to the coordination mode of the 9-methyladenine. In compound 1, which seems to be the kinetically favored one, the isophthalato ligand exhibits a $\mu\text{-}\kappa^2\text{O},\text{O}':\kappa\text{O}''$ coordination mode giving rise to a 4 + 1 + 1 copper(II) environment. The carboxylate groups only form a strong coordination bond with the metal center through one of their oxygen atoms, whereas the remaining ones are semicoordinated (O21) or remain free (O12) due to the steric hindrance of the coordinated water molecules. However, more prolonged crystallization times or small temperature changes lead to the loss of the coordination water molecules that induces a slight modification of the coordination sphere giving rise to two four-member chelate rings through its $\mu\text{-}\kappa^2\text{O},\text{O}':\kappa^2\text{O}'',\text{O}'''$ coordination mode. This new arrangement folds the copper(II)-isophthalato chains by forcing consecutive isophthalato ligands to be perpendicular to

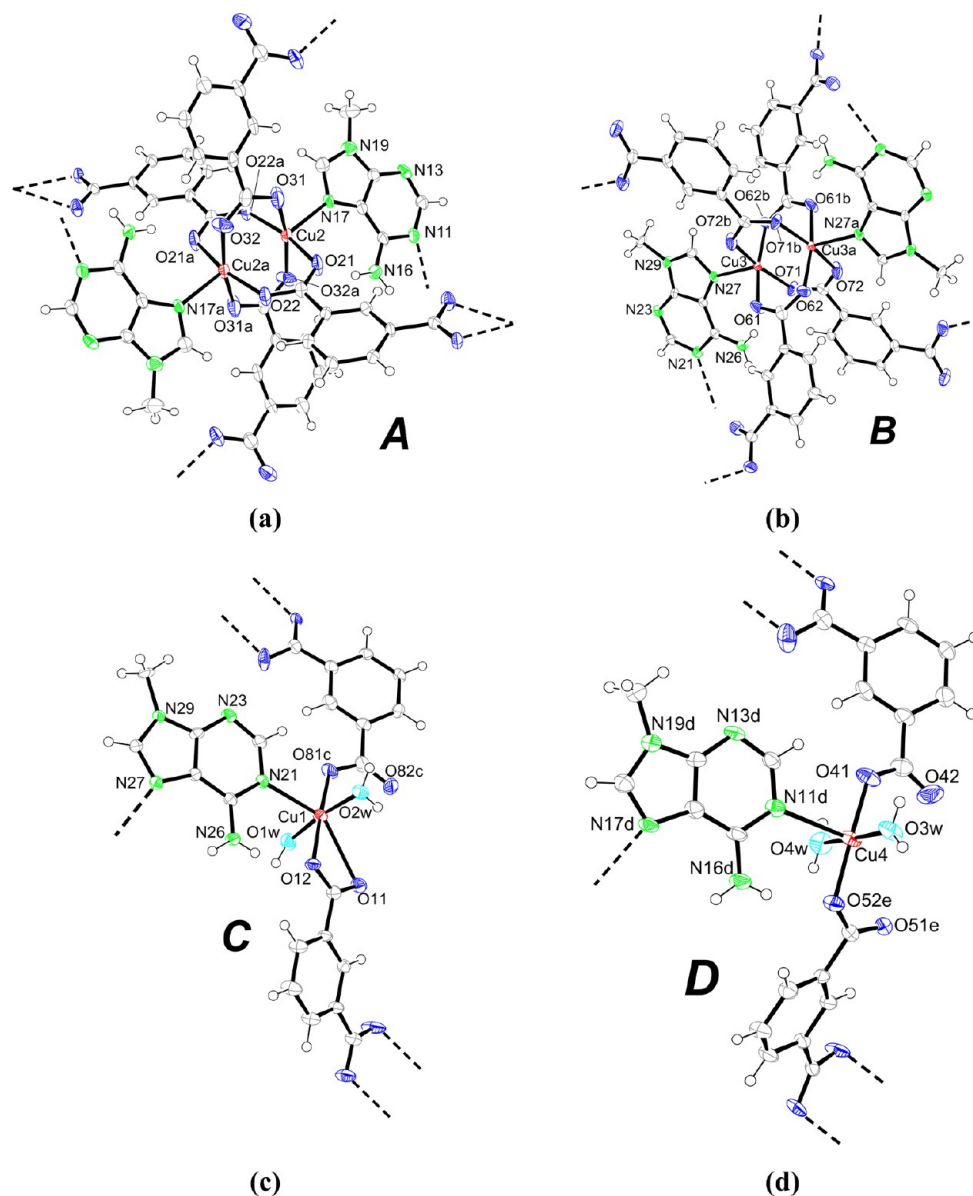


Figure 12. (a–d) Structural entities in compound 5.

Table 6. Selected Bond Lengths (Å) of Compound 5^a

coordination environments in the dimeric entities			
Cu2–N17	2.205(5)	Cu3–N27	2.156(4)
Cu2–O21	1.953(4)	Cu3–O61	1.961(4)
Cu2–O22a	1.957(4)	Cu3–O62b	1.969(4)
Cu2–O31	1.959(5)	Cu3–O71	1.974(4)
Cu2–O32a	1.970(5)	Cu3–O72b	1.955(4)
Cu2...Cu2a	2.716(2)	Cu3...Cu3b	2.670(1)
coordination environments in the monomeric entities			
Cu1–N21	2.373(4)	Cu4–N11d	2.498(5)
Cu1–O11	2.677(4)	Cu4–O41	1.906(4)
Cu1–O12	1.936(4)	Cu4–O52e	1.941(4)
Cu1–O81c	1.912(4)	Cu4–O3w	2.004(4)
Cu1–O1w	2.060(5)	Cu4–O4w	1.980(4)
Cu1–O2w	2.036(4)		

^aSymmetry codes: (a) $-x + 1, -y, -z + 1$; (b) $-x + 2, -y, -z$; (c) $x, y + 1, z$; (d) $-x + 1, -y + 1, -z + 1$; (e) $-x + 2, -y + 1, -z + 1$.

each other. The 9-methyladenine can, in this way, coordinate the metal centers of neighboring chains in a N1,N7-bidentate fashion, which renders the 2D network of compound 2.

In compound 3, the isophthalato ligand adopts its most usual $\mu_4\text{-}\kappa\text{O}:\kappa\text{O}':\kappa\text{O}'':\kappa\text{O}'''$ coordination mode to give 2D layers built up from PW entities in which the 9-methyladenine- $\kappa\text{N}7$ ligand, as predicted, occupies the apical position. The isophthalato ligands, in compounds 4 and 5, adopt again nonsymmetric coordination modes ($\mu_3\text{-}\kappa\text{O}:\kappa\text{O}':\kappa^2\text{O}'',\text{O}'''$ and $\mu_3\text{-}\kappa\text{O}:\kappa\text{O}':\kappa\text{O}''$) which prevent the formation of PW entities solely, in such a way that the PW entities are linked through monomeric ones. This coordination scheme allows the 9-methyladenine to join the building units together by the N1,N7-bidentate bridge.

At this point, it becomes evident that in the reaction media the predicted $[\text{Cu}_2(\mu\text{-iso})_4(9\text{Meade})_2]$ unit coexists with different monomeric entities, whose combination leads to the structural diversity herein reported. The segregation of the kinetically favored compound 1 during the crystallization process alters the concentration and ratio between the building units giving access to the remaining crystal structures. In fact,

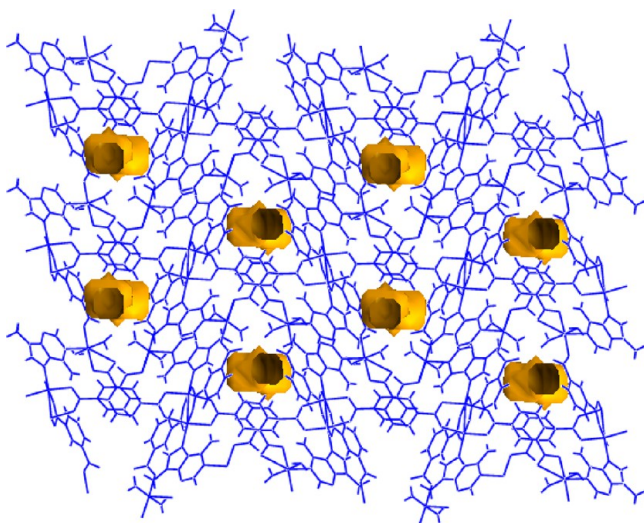


Figure 13. Crystal packing of compound **5** showing the voids occupied by crystallization water molecules.

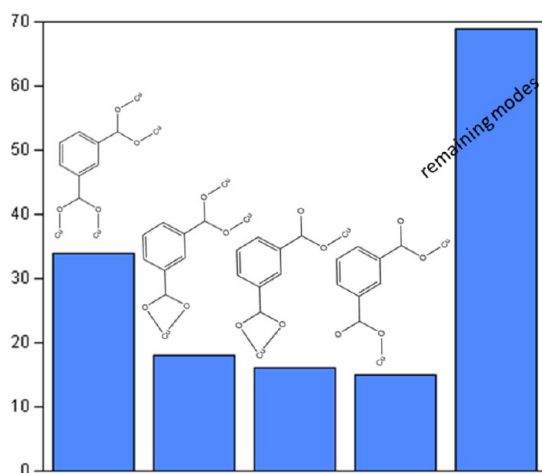


Figure 14. Most frequent isophthalate coordination modes in copper(II) complexes.

compounds **1** and **2** are grown by the assembly of monomeric: $[\text{Cu}(\text{OH})_2(\text{iso})_2(9\text{Meade})]$ and $[\text{Cu}(\text{iso})_2(9\text{Meade})_2]$ building blocks, while compound **3** is built up by the linkage of $[\text{Cu}_2(\mu\text{-iso})_4(9\text{Meade})_2]$ units, and compounds **4** and **5** are composed of both monomeric and dimeric entities. Therefore, this kinetically labile system represents an example of the reversible combination of the initial metal ions and ligands to form a dynamic combinatorial library from which the final crystal structures emerge.²⁴

It must be pointed out that this behavior arises mainly from the coordination versatility of copper(II). In fact, the use of metal centers with predominant coordination environments reduces the structural variability. Evidence is provided by the reaction of nickel(II) with isophthalic acid and adenine under hydrothermal conditions, which only affords one compound isorecticular to **2** with all metal centers hexacoordinated.²⁵

CONCLUSIONS

The present work shows the achievement of building metal-biomolecule frameworks employing isophthalato and 9-methyladenine. The aromatic dicarboxylic rigid dianion acts as bridging ligand in all compounds leading to architectures that

range from 1D to 3D frameworks. It becomes obvious that there are many energetically available architectures for this system based on the slight modifications of the Cu^{II} /isophthalato/adenine ratio, temperature, and pH value that take place both along the diffusion test tube and during the experiment progress. It is also notorious that although the 9-methyladenine nucleobase usually behaves as an N7-terminal ligand, in some of these compounds (**2**, **4**, and **5**) it is also able to bridge adjacent metal centers showing a $\mu\text{-}\kappa\text{N1}:\kappa\text{N7}$ -coordination mode. Further work is in progress to achieve analogous compounds with other benzenedicarboxylates such as terephthalic, aminoterephthalic, and chloroterephthalic acids.

ASSOCIATED CONTENT

Supporting Information

Tables and figures of noncovalent interactions, and crystallographic information files (CIF). This information is available free of charge via the Internet at <http://pubs.acs.org>.

AUTHOR INFORMATION

Corresponding Author

*E-mail: sonia.perez@ehu.es (S.P.-Y.), oscar.castillo@ehu.es (O.C.). Fax: (internat) +34-94601-3500.

Notes

The authors declare no competing financial interest.

ACKNOWLEDGMENTS

Financial support from the Gobierno Vasco (IT477-10, SAIOTEK S-PE12UN004) and the Universidad del País Vasco/Euskal Herriko Unibertsitatea (UFI 11/S3, postdoctoral fellowship) is gratefully acknowledged. Technical and human support provided by SGIker (UPV/EHU, MICINN, GV/EJ, ESF) is also acknowledged.

REFERENCES

- (1) (a) Amo-Ochoa, P.; Sanz Miguel, P. J.; Castillo, O.; Houlton, A.; Zamora, F. In *Metal Complex-DNA Interactions*; Hadjiladis, N.; Sletten, E., Eds. Wiley: Chichester, 2009; Chapter 4, pp 95–132. (b) Castillo, O.; Luque, A.; García-Terán, J. P.; Amo-Ochoa, P.; In *Macromolecules Containing Metal and Metal-Like Elements*; Abd-el-Aziz, A. S.; Carraher, C. E.; Pittman, C. U.; Zeldin, M., Eds. Wiley & Sons: Hoboken, 2009; Vol. 9, Chapter 9, pp 407–449. (c) An, J.; Geib, S. J.; Rosi, N. L. *J. Am. Chem. Soc.* **2010**, *132*, 38. (d) Verma, S.; Mishra, A. K.; Kumar, A. *Acc. Chem. Res.* **2010**, *43*, 79.
- (2) (a) MacGillivray, L. In *Metal-Organic Frameworks: Design and Application*; John Wiley and Sons: New York, 2010. (b) Meek, S. T.; Greathouse, J. A.; Allendorf, M. D. *Adv. Mater.* **2011**, *23*, 249. (c) Köberl, M.; Cokoja, M.; Hermann, W. A.; Kühn, F. E. *Dalton Trans.* **2011**, *40*, 6834. (d) Carné, A.; Carbonell, C.; Imaz, I.; Maspocho, D. *Chem. Soc. Rev.* **2011**, *40*, 291. (e) Mas-Ballesté, R.; Gómez-Herrero, J.; Zamora, F. *Chem. Soc. Rev.* **2010**, *39*, 4220. (f) Givaja, G.; Amo-Ochoa, P.; Gómez-García, C. J.; Zamora, F. *Chem. Soc. Rev.* **2012**, *41*, 115.
- (3) (a) Bleany, B.; Bowers, K. D. *Proc. R. Soc. London Ser. A.* **1952**, *214*, 451. (b) Van Niekerk, J. B.; Schoening, F. R. L. *Acta Crystallogr.* **1953**, *6*, 227.
- (4) Abourahma, H.; Badwell, G. J.; Lu, J.; Moulton, B.; Pottie, I. R.; Walsh, R. B.; Zaworotko, M. J. *Cryst. Growth Des.* **2003**, *3*, 513.
- (5) (a) Vagin, S. I.; Ott, A. K.; Rieger, B. *Chem. Ing. Tech.* **2007**, *79*, 767. (b) Chen, B.; Xiang, S.; Quian, G. *Acc. Chem. Res.* **2010**, *43*, 1115. (c) Zhao, D.; Timmons, D. J.; Yuan, D.; Zhou, H. C. *Acc. Chem. Res.* **2011**, *44*, 123.
- (6) Leong, W. L.; Vittal, J. J. *Chem. Rev.* **2011**, *111*, 688.
- (7) Eddaoudi, M.; Kim, J.; Rosi, N.; Vodak, D.; Wachter, J.; O'Keeffe, M.; Yaghi, O. M. *Science* **2002**, *295*, 469.

- (8) (a) An, J.; Geib, S. J.; Rosi, N. L. *J. Am. Chem. Soc.* **2009**, *131*, 8367. (b) An, J.; Rosi, N. L. *J. Am. Chem. Soc.* **2010**, *132*, 5578. (c) Stylianou, K. C.; Warren, J. E.; Chong, S. Y.; Rabone, J.; Bacsá, J.; Bradshaw, D.; Rosseinsky, M. J. *Chem. Commun.* **2011**, *47*, 3389. (d) An, J.; Shade, C. M.; Chengelis-Czegan, D. A.; Petoud, S.; Rosi, N. L. *J. Am. Chem. Soc.* **2011**, *133*, 1120.
- (9) Beobide, G.; Castillo, O.; Cepeda, J.; Luque, A.; Pérez-Yáñez, S.; Román, P.; Thomas-Gipson, J. *Coord. Chem. Rev.* **2013**, DOI: 10.1016/j.ccr.2013.03.011.
- (10) Pérez-Yáñez, S.; Beobide, G.; Castillo, O.; Cepeda, J.; Luque, A.; Román, P. *Cryst. Growth Des.* **2012**, *12*, 3324.
- (11) Devic, T.; Horcajada, P.; Serre, C.; Salles, F.; Maurin, G.; Moulin, B.; Heurtaux, D.; Clet, G.; Vimont, A.; Grenèche, J.-M.; Le Ouay, B.; Moreau, F.; Magnier, E.; Filinchuk, Y.; Marrot, J.; Lavalley, J.-C.; Daturi, M.; Férey, G. *J. Am. Chem. Soc.* **2010**, *132*, 1127.
- (12) (a) Ke, Y.; Collins, D. J.; Zhou, H. —C. *Inorg. Chem.* **2005**, *44*, 4154. (b) Eddaoudi, M.; Kim, J.; Wachter, J. B.; Chae, H. K.; O’Keeffe, M. O.; Yaghi, O. M. *J. Am. Chem. Soc.* **2001**, *123*, 4368. (c) Li, J.-R.; Zhou, H.-C. *Nat. Chem.* **2010**, *2*, 893. (d) Moulton, B.; Lu, J.; Mondal, A.; Zaworotko, M. J. *Chem. Commun.* **2001**, 863.
- (13) (a) Xue, D.-X.; Lin, Y.-Y.; Cheng, X.-N.; Chen, X.-M. *Cryst. Growth Des.* **2007**, *7*, 1332. (b) Bourne, S. A.; Lu, J.; Mondal, A.; Moulton, B.; Zaworotko, M. J. *Angew. Chem., Int. Ed.* **2001**, *40*, 2111. (c) Zhong, R.-Q.; Zou, R.-Q.; Xu, Q. *CrystEngComm* **2011**, *13*, 577.
- (14) Chun, H.; Jung, H.; Seo, J. *Inorg. Chem.* **2009**, *48*, 2043.
- (15) STAD14 and X-RED; Stoe & Cie GmbH: Darmstadt, Germany, 2002.
- (16) CrysAlis, RED, version 1.170; Oxford Diffraction: Wroclaw, Poland, 2003.
- (17) Altomare, A.; Cascarano, M.; Giacovazzo, C.; Guagliardi, A. J. *Appl. Crystallogr.* **1993**, *26*, 343.
- (18) Sheldrick, G. M. *Acta Crystallogr.* **2008**, A64, 112.
- (19) Farrugia, L. J. WINGX, A Windows Program for Crystal Structure Analysis; University of Glasgow: Glasgow, Great Britain, 1998.
- (20) (a) Llunel, M.; Casanova, D.; Cirera, J.; Bofill, J. M.; Alemany, P.; Alvarez, S.; Pinsky, M.; Avnir, D. SHAPE (1.7); University of Barcelona: Barcelona, 2010. (b) Ruiz-Martínez, A.; Casanova, D.; Alvarez, S. *Chem.—Eur. J.* **2008**, *14*, 1291.
- (21) (a) Schreiber, A.; Hillgeris, E. C.; Lippert, B. Z. *Naturforsch. B. Chem. Sci.* **1993**, *48*, 1603. (b) McCall, M. J.; Taylor, M. R. *Acta Crystallogr.* **1976**, B32, 1687. (c) Sigel, R. K. O.; Thompson, S. M.; Freisinger, E.; Glahe, F.; Lippert, B. *Chem.—Eur. J.* **2001**, *7*, 1968. (d) Luth, M. S.; Freisinger, E.; Lippert, B. *Chem.—Eur. J.* **2001**, *7*, 2104. (e) Luth, M. S.; Freisinger, E.; Glahe, F.; Lippert, B. *Inorg. Chem.* **1998**, *37*, 5044. (f) Luth, M. S.; Freisinger, E.; Glahe, F.; Muller, J.; Lippert, B. *Inorg. Chem.* **1998**, *37*, 3195. (g) Jaworski, S.; Menzer, S.; Lippert, B.; Sabat, M. *Inorg. Chim. Acta* **1993**, *205*, 31. (h) Rother, I. B.; Freisinger, E.; Erxleben, A.; Lippert, B. *Inorg. Chim. Acta* **2000**, *300*, 339. (i) Roitzsch, M.; Rother, I. B.; Willermann, M.; Erxleben, A.; Costisella, B.; Lippert, B. *Inorg. Chem.* **2002**, *41*, 5946. (j) Rother, I. B.; Willermann, M.; Lippert, B. *Supramol. Chem.* **2002**, *14*, 189.
- (22) (a) Blatov, V. A.; Schevchenko, A. P. TOPOS v4.0; Samara State University: Samara, 2011. (b) Blatov, V. A. *IUCr CompComm. Newslett.* **2006**, *7*, 4. (c) Blatov, V. A.; O’Keeffe, M.; Proserpio, D. M. *CrystEngComm* **2010**, *12*, 44.
- (23) Allen, F. H. *Acta Crystallogr. Sect. B* **2002**, *58*, 380.
- (24) Corbett, P. T.; Leclaire, J.; Vial, L.; West, K. R.; Wietor, J.-L.; Sanders, J. K. M.; Otto, S. *Chem. Rev.* **2006**, *106*, 3652.
- (25) Huang, H.-X.; Tian, X.-Z.; Song, Y.-M.; Liao, Z.-W.; Sun, G.-M.; Luo, M.-B.; Liu, S.-J.; Xu, W.-Y.; Luo, F. *Aust. J. Chem.* **2012**, *65*, 320.